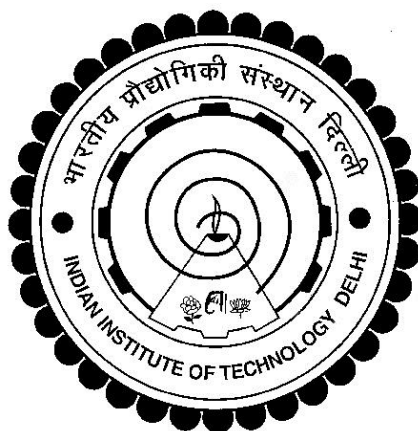


**STUDIES ON THE FOAMING BEHAVIOUR OF SEBS BASED
BLENDS AND NANOCOMPOSITES**

RITIMA BANERJEE



DEPARTMENT OF MATERIALS SCIENCE AND ENGINEERING

INDIAN INSTITUTE OF TECHNOLOGY DELHI

JULY 2018

©Indian Institute of Technology Delhi (IITD), New Delhi, 2018

STUDIES ON THE FOAMING BEHAVIOUR OF SEBS BASED BLENDS AND NANOCOMPOSITES

by

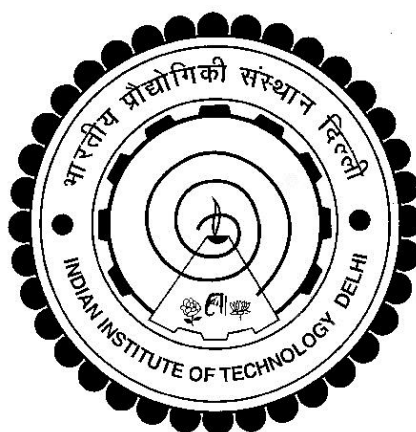
RITIMA BANERJEE

Department of Materials Science and Engineering

Submitted

in fulfillment of the requirements of the degree of Doctor of Philosophy

to the



INDIAN INSTITUTE OF TECHNOLOGY DELHI

JULY 2018

Dedicated with deep adoration to the Supreme Lord

Certificate

This is to certify that the thesis entitled “**Studies on the foaming behaviour of SEBS based blends and nanocomposites**” being submitted by **Ms. Ritima Banerjee** to the Indian Institute of Technology Delhi, for the fulfillment of award of the degree “**Doctor of Philosophy**” is a record of bonafide research work carried by her under our supervision. This thesis has been prepared in conformity with the rules and regulations of the Indian Institute of Technology Delhi, New Delhi. We further certify that the thesis has attained a standard required for a Ph.D. degree of the institute. The research reported and results presented in the thesis have not been submitted in part or full to any other institute or university for the award of any other degree or diploma.

(Anup K Ghosh)

Professor and Head
Department of Materials Sc. & Engg.
Indian Institute of Technology Delhi
Hauz Khas, New Delhi-110016, India



(Suprakas Sinha Ray)

Chief Research Scientist and Director
DST/CSIR Nanotechnology Innovation Centre
National Centre for Nanostructured Materials
CSIR, Pretoria-0001, South Africa

Acknowledgements

This thesis is a result of four years of work, during which I was fortunate to receive the support of many individuals. It gives me immense pleasure to express my gratitude to all of them.

Foremost, I would like to express my sincere gratitude to my supervisors Prof. Anup K Ghosh and Prof. Suprakas Sinha Ray for guiding me all the way during my PhD tenure. Their patience, motivation, enthusiasm and immense knowledge have helped me overcome all challenges and move forward towards my goal. They have always encouraged me to put in extra efforts and have made me aware of my own potential. I have learnt from them that stumbling blocks should strengthen one's will power and provide the motivation to work harder. I am grateful to them for nurturing in me qualities, which not only helped me during my PhD tenure, but will propel me forward in all future endeavours of my life.

I am grateful to my research committee members Prof. Manjeet Jassal, Dr. Bhabani K. Satapathy and Prof. Naresh Bhatnagar for monitoring my work and providing their valuable suggestions. I would also like to thank Prof. S.N. Maity, Prof. Veena Chaudhary, Prof. Josemon Jacob, Dr. Leena Nebhani, Dr. Sampa Saha and Dr. Bijay Tripathi, who despite their busy schedule have always been happy to provide their guidance and support.

I would like to convey my special thanks to Ms. Deepika Malpani for her valuable suggestions in rheological analysis.

This work would not have been possible without the support and encouragement of my lab-mates, seniors and juniors. I am indebted to Dr. Tahir Zafar and Dr. Priyanka Singh for sharing with me their experience and knowledge. Dr. Zafar deserves my special thanks for his help in formatting and proofreading my thesis. I am grateful to Dr. Rajendra Singla, Dr. Astha Garhwal and Ms. Achla for extending their support whenever I sought their help. I owe thanks to Anindya and Sabapathy for the stimulating discussions we had while working together. I would also like to thank Harshita, Swarna, Prajesh, Srijita, Bariya, Ashok, Devendra, Agni, Pragati, Debang, Ranjana, Shilpi, Sampat, Banpreet, Sumbul, Ifra, Sucharita, Smruti and Saheli for the fun we had during my stay in IIT.

I am grateful to the laboratory staff members Mr. Surender Sharma, Mr. Ashok Kapoor, Mr. Shiv Kant, Mr. Ehteshamul Islam and Mr. Gajraj Singh for their technical assistance. Mr. Islam took a keen interest in my work, enriching me with his expertise in polymer processing

operations. I do not have enough words to describe how much I appreciate his help. Mr. Kuldeep Singh and Ms. Kumud Arora deserve my special thanks for their support in carrying out SEM studies. I would also like to thank Ms. Shalini Arora, Mr. Narender Kumar, Mr. Sudheer Pandey and Mr Pramod Kale for reaching out with all kinds of support whenever I needed help.

I would like to acknowledge the Ministry of Human Resources Development (MHRD), Government of India, for providing me with scholarship during my entire PhD tenure.

I take this opportunity to express my deep gratitude to my family members. I do not have enough words to thank my parents (Late Mitra Banerjee and Late Gautam Banerjee), who with their unconditional love and support, nurtured in me the qualities required to undertake and complete this project. The debt of gratitude I owe them is immeasurable. I am grateful to my uncle (Dr. Arun Chatterjee) and my aunts (Dr. Gopa Bhattacharya, Dr. Sati Mazumdar, Mrs. Kalpana Chatterjee and Mrs. Saumya Chatterjee) for their constant moral support and encouragement.

This acknowledgement will not be complete if I do not recognize the contribution of my dear friend Ankana. Ankana was by my side at all times, boosting my confidence, helping me tide over difficulties, rejoicing at my success and encouraging me to perform better. One of the greatest gifts in my life is my friendship with her.

I would specially like to thank "Little Rik" for showering me with his love and making my life more fulfilling, which enhanced my performance at work.

Finally and above all, I thank the Supreme Lord for His ocean of Grace, without which my academic pursuit would not have been successful.

Date:

(Ritima Banerjee)

Abstract

Styrene-ethylene-butylene-styrene/polystyrene blends (containing 10, 20, 30 and 50 wt % polystyrene) and styrene-ethylene-butylene-styrene nanocomposites (containing 0.5, 1, 2 and 4 wt% Cloisite[®] 20A) were melt compounded, injection moulded, characterised and subsequently foamed.

Scanning electron microscopy of the blends in back-scattered imaging mode revealed that a portion of the added polystyrene was miscible with the styrene blocks of styrene-ethylene-butylene-styrene (SEBS), thereby increasing the domain size whereas the remaining portion got phase separated forming micrometer-sized aggregates. Blends with a higher polystyrene (PS) content (30 and 50 wt% polystyrene) possessed a fibrillar morphology, resulting in a remarkable increase in tensile modulus and storage modulus (in dynamic mechanical analysis).

The nanocomposites exhibited a mixed morphology in transmission electron microscopy. The clay was dispersed in both the polystyrene and the elastomeric phases, as indicated by shift in $\tan \delta$ peak of both phases in dynamic mechanical analysis. An increase in clay content resulted in an increased formation of agglomerates as well as 3D mesoscopic structures. The nanocomposite with 1 wt% nanoclay exhibited maximum intercalation and delamination, with minimum agglomeration, resulting in maximum tensile modulus and storage modulus (in dynamic mechanical analysis).

The compositions were batch foamed using carbon dioxide. The foaming behaviour of both blends and nanocomposites depended on material characteristics and foaming temperature. At foaming temperatures close to the glass transition temperature of the polystyrene phase, when foaming of both the polystyrene and the ethylene-butylene phases occurred, compositions with higher storage modulus and complex viscosity produced foams of higher volume expansion ratio and lower shrinkage. However, unlike foams of the blends, where shrinkage was completely eliminated in case of blends of a higher polystyrene content, foams of all the nanocomposites shrank. But shrinkage of all nanocomposite foams was significantly lower than that of neat SEBS foam. Also, nanocomposites with well-dispersed nanoclay produced foams having morphology superior to that of foams of the blends, attributed to enhancement of melt strength and occurrence of heterogeneous nucleation by the nanofiller,

At foaming temperatures close to room temperature, the elastomeric phase was selectively foamed. The polystyrene particles (polystyrene domains of the copolymer and phase separated

aggregates of the blends) and the nanoclay in the elastomeric phase (in case of nanocomposites) served as sites of heterogeneous nucleation. Irrespective of rheological properties, all foams showed prominent shrinkage. Greater the number of polystyrene particles (in case of the blends) or the stiffness of the polystyrene phase (in nanocomposites, due to the dispersed clay), lower was the volume expansion ratio and higher was the shrinkage.

For a given composition, the quality of dispersion, as well as the foaming behaviour of both blends and nanocomposites depended on the primary processing conditions employed during compounding. In case of blends, a lower screw speed (around 100 rpm in a 16 mm twin screw extruder) favoured a finer quality of dispersion of the polystyrene particles. In case of nanocomposites, a screw speed of around 200 rpm resulted in superior quality of dispersion of nanoclay without degradation of the matrix. The blends and nanocomposites produced at 100 rpm and 200 rpm respectively, exhibited better tensile and rheological properties, as well as enhanced foamability at both higher and lower foaming temperatures.

In order to understand whether a synergistic combination of the attributes of the blend foams and the nanocomposite foams can be achieved in foams of ternary compositions, ternary compositions containing 30 wt% polystyrene and 1 wt% nanoclay were prepared and foamed at 100 °C. Though the foams exhibited no shrinkage and had superior volume expansion ratio, morphology was poor, as in case of foams of blends.

सार

स्टायरिन-एथिलीन-ब्यूटिलीन-स्टायरिन / पॉलीस्टीरिन मिश्रण (जिसमें 10, 20, 30 और 50 वाट% पॉलीस्टीरिन युक्त) और स्टायरिन-एथिलीन-ब्यूटिलीन-स्टायरिन नैनोकोमोसाइट्स (0.5, 1, 2 और 4 वाट% क्लॉसाइट 20 ए युक्त) मिश्रित पिघल गए थे, इंजेक्शन मोल्ड, विशेषता और बाद में foamed।

बैक-बिखरे हुए इमेजिंग मोड में मिश्रणों के इलेक्ट्रॉन माइक्रोस्कोपी स्कैनिंग से पता चला है कि जोड़ा पॉलीस्टीरिन का एक हिस्सा स्टायरिन-एथिलीन-ब्यूटिलीन-स्टायरिन (एसईबीएस) के स्टायरिन ब्लॉक के साथ मिस्सीबल था, जिससे डोमेन आकार में वृद्धि हुई जबकि शेष हिस्से को चरण अलग किया गया माइक्रोमीटर आकार के योग बनाते हैं। एक उच्च पॉलीस्टीरिन (पीएस) सामग्री (30 और 50 वाट% पॉलीस्टीरिन) के साथ मिश्रणों में एक फाइब्रिलर मॉर्फोलॉजी है, जिसके परिणामस्वरूप तन्यता मॉड्यूलस और स्टोरेज मॉड्यूलस (गतिशील यांत्रिक विश्लेषण में) में उल्लेखनीय वृद्धि हुई है।

नैनोकोमोसाइट्स ने ट्रांसमिशन इलेक्ट्रॉन माइक्रोस्कोपी में एक मिश्रित रूपरेखा प्रदर्शित की। मिट्टी को पॉलीस्टीरिन और elastomeric चरणों दोनों में फैल गया था, जैसा गतिशील यांत्रिक विश्लेषण में दोनों चरणों के तन δ चोटी में बदलाव द्वारा इंगित किया गया है। मिट्टी की सामग्री में वृद्धि के परिणामस्वरूप एग्लोमेरेट्स के साथ-साथ 3 डी मेसोस्कोपिक संरचनाओं में वृद्धि हुई। 1 वाट% नैनोकले के साथ नैनोकोमोसाइट ने अधिकतम संचलन और संदूषण का प्रदर्शन किया, न्यूनतम समूह के साथ, जिसके परिणामस्वरूप अधिकतम तन्यता मॉड्यूलस और स्टोरेज मॉड्यूलस (गतिशील यांत्रिक विश्लेषण में) होता है।

कार्बन डाइऑक्साइड का उपयोग करके संरचनाओं को बैच फोमिंग किया गया था। दोनों मिश्रणों और नैनोकोमोसाइट्स का फोमिंग व्यवहार भौतिक विशेषताओं और फोमिंग तापमान पर निर्भर करता है। पॉलीस्टीरिन चरण के ग्लास संक्रमण तापमान के करीब फोमिंग तापमान पर, जब पॉलीस्टीरिन और ईथिलीन-ब्यूटिलीन चरण दोनों का फोमिंग हुआ, उच्च भंडारण मॉड्यूलस और जटिल चिपचिपाहट के साथ रचनाओं ने उच्च मात्रा विस्तार अनुपात और कम संकोचन के फॉम्स का उत्पादन किया। हालांकि, मिश्रणों के फोम के विपरीत, जहां उच्च पॉलीस्टीरिन सामग्री के मिश्रणों के मामले में संकोचन पूरी तरह समाप्त हो गया था, सभी नैनोकोमोसाइट्स के फॉम्स गिर गए। लेकिन सभी नैनोकोमोसाइट्स फॉम्स का संकोचन साफ सेब एसईबीएस फोम की तुलना में काफी कम था। इसके अलावा, अच्छी तरह फैलाने वाले नैनोकले के साथ नैनोकोमोसाइट्स

ने फोमों को मोर्फोलॉजी के मिश्रणों से बेहतर रूप से विकसित किया है, जो पिघलने की शक्ति में वृद्धि और नैनोफिलर द्वारा विषम न्यूक्लियेशन की घटना के कारण जिम्मेदार है,

कमरे के तापमान के करीब फोमिंग तापमान पर, इलास्टोमेरिक चरण को चुनिंदा रूप से फोम किया गया था। पॉलीस्टीरिन कण (कोपोलिमर के पॉलीस्टीरिन डोमेन और मिश्रण मिश्रणों के चरण अलग-अलग होते हैं) और इलास्टोमेरिक चरण (नैनोकोमोसाइट्स के मामले में) में नैनोकले विषम न्यूक्लियेशन की साइट के रूप में कार्य करता है। भौतिक गुणों के बावजूद, सभी फूमस ने प्रमुख संकोचन दिखाया। पॉलीस्टीरिन कणों (मिश्रणों के मामले में) या पॉलीस्टीरिन चरण (नैनोकोमोसाइट्स में, फैलाने वाली मिट्टी के कारण) की कठोरता जितनी अधिक होती है, मात्रा कम होने का अनुपात कम होता है और उच्च संकुचन होता है।

किसी दिए गए रचना के लिए, फैलाव की गुणवत्ता, साथ ही मिश्रण और नैनोकोमोसाइट्स दोनों के फोमिंग व्यवहार परिसर के दौरान नियोजित प्राथमिक प्रसंस्करण स्थितियों पर निर्भर थे। मिश्रणों के मामले में, एक निचली पेंच गति (16 मिमी जुड़वां पेंच extruder में लगभग 100 आरपीएम) polystyrene कणों के फैलाव की एक बेहतर गुणवत्ता का पक्ष लिया। नैनोकोमोसाइट्स के मामले में, लगभग 200 आरपीएम की एक स्कू की गति के परिणामस्वरूप मैट्रिक्स के अवक्रमण के बिना नैनोकले के फैलाव की बेहतर गुणवत्ता होती है। क्रमशः 100 आरपीएम और 200 आरपीएम पर उत्पादित मिश्रण और नैनोकोमोसाइट्स, बेहतर तन्यता और भौतिक गुणों के साथ-साथ उच्च और निम्न फोमिंग तापमान दोनों में बढ़ी हुई फोमबिलिटी प्रदर्शित करते हैं।

यह समझने के लिए कि क्या मिश्रण फूमस और नैनोकोमोसाइट फॉम्स के गुणों का एक सहक्रियात्मक संयोजन टर्नरी रचनाओं के फोम में हासिल किया जा सकता है, 30 वाट% पॉलीस्टीरिन युक्त टर्नरी संरचनाएं और 1 वाट% नैनोकले तैयार की जाती हैं और 100 डिग्री सेल्सियस पर फॉम्ड होती हैं। हालांकि फॉम्स ने कोई संकोचन नहीं किया और बेहतर मात्रा विस्तार अनुपात था, मिश्रणों के फोम के मामले में रूपरेखा खराब थी।

Contents

	Page Number
List of Figures	i
List of Tables	vi
List of Symbols	viii
List of Abbreviations	ix
Chapter 1 Introduction and Literature Survey	
1.1 Preamble	1
1.1.1 SEBS/PS blends and SEBS nanocomposites	2
1.1.2 Highlights of the present work	3
1.2 Thermoplastic elastomers	4
1.2.1 Types and applications	4
1.2.2 Key players and market estimates	6
1.3 Polymer blends	6
1.3.1 Basics of polymer blends and their types	6
1.3.2 Morphology of immiscible blends	7
1.3.3 Role of processing conditions in blend morphology	8
1.4 Polymer nanocomposites	9
1.4.1 Basics of polymer nanocomposites and layered silicate nanocomposites	9
1.4.2 Morphology of layered silicate nanocomposites	12
1.4.3 Challenges in the production of layered silicate nanocomposites	13
1.4.4 Preparation of layered silicate nanocomposites	15
1.4.4.1 In-situ intercalative polymerization	15

1.4.4.2	Intercalation of polymer or prepolymer	
	from solution	15
1.4.4.3	Melt intercalation	15
1.4.5	Role of processing conditions in melt processing of nanocomposites	16
1.5	Rheology as a tool for assessing morphology	17
1.6	Foaming of polymers	19
1.6.1	Basics of foams, foaming and polymeric foams	19
1.6.2	Blowing agents	21
1.6.3	Foam manufacturing techniques	21
	1.6.3.1 Batch foaming	22
	1.6.3.2 Extrusion foaming	23
	1.6.3.3 Foam injection moulding	24
1.6.4	Properties and applications of polymeric foams	24
1.6.5	Key players and market estimates	26
1.7	Foaming behaviour of polymeric materials	26
1.7.1	Material characteristics influencing foaming behaviour	28
	1.7.1.1 Rheological characteristics	29
	1.7.1.1.1 Dynamic rheology	29
	1.7.1.1.2 Extensional rheology	30
	1.7.1.1.3 Shear rheology	31
1.7.1.2	Morphological characteristics	32
	1.7.1.2.1 Crystallinity	32
	1.7.1.2.2 Heterogeneous nucleating agents	32
1.7.1.3	Correlation of rheology and morphology in	

	foaming behaviour	35
	1.7.2 Processing conditions influencing foaming behaviour	35
	1.7.3 Influence of blowing agent on foaming behaviour	39
	1.7.4 Foaming of polymer blends and nanocomposites	40
	1.7.5 Shrinkage of polymer foams	40
	1.7.6 Summary	41
1.8	Objective	43
1.9	Format of thesis	44
	<i>References</i>	47
Chapter 2	Materials and Methods	
2.1	Introduction	64
2.2	Raw materials	64
	2.2.1 SEBS	64
	2.2.2 PS	64
	2.2.3 SEBS-g-MA	65
	2.2.4 Cloisite 20A	65
2.3	Compositions	66
2.4	Methods	67
	2.4.1 Compounding and shear rheology in micro-compounder	67
	2.4.2 Extrusion	68
	2.4.3 Injection moulding	68
	2.4.4 Differential scanning calorimetry	68
	2.4.5 Thermal gravimetric analysis	68
	2.4.6 Tensile testing	69

2.4.7	Dynamic mechanical analysis	69
2.4.8	Melt state dynamic rheology	70
2.4.9	Wide angle X-ray diffraction studies	70
2.4.10	Transmission electron microscopy	70
2.4.11	Batch foaming	71
2.4.12	Scanning electron microscopy	71
2.4.13	Density measurements	71
2.4.14	Analysis of shrinkage of foams	72
2.4.15	ImageJ analysis	73
	<i>References</i>	73

Chapter 3 Morphological, Mechanical, Thermal and Rheological Properties of SEBS/PS Blends

3.1	Introduction	75
3.2	Effect of compositional variation	76
3.2.1	Blend sample preparation and torque measurements	76
3.2.2	SEM studies	77
3.2.3	Tensile properties	83
3.2.4	DMA studies	88
3.2.5	Thermal characterisation	90
	3.2.5.1 DSC studies	90
	3.2.5.2 TGA studies	93
3.2.6	Melt state dynamic rheology	94
3.2.7	Shear rheology	97
3.2.8	Energy requirements for processing	101

3.3	Effect of screw speed	101
3.3.1	Blend sample preparation and residence time determination	102
3.3.2	Melt state rheology	103
3.3.3	SEM studies	106
3.3.4	Tensile test	107
3.3.5	DMA studies	109
3.4	Conclusions	110
	<i>References</i>	111
Chapter 4	Foaming Behaviour of SEBS/PS Blends	
4.1	Introduction	116
4.2	Effect of compositional variation	117
4.2.1	Batch foaming	117
4.2.1.1	Shrinkage of foams with time	118
4.2.1.2	SEM studies of foams	124
4.2.1.2.1	Foaming temperature of 35 °C	124
4.2.1.2.2	Higher foaming temperatures	127
4.3	Effect of screw speed	128
4.3.1	Batch foaming	129
4.3.1.1	Shrinkage of foams with time	129
4.3.1.2	SEM studies of foams	132
4.3.1.2.1	Foaming temperature of 35 °C	133
4.3.1.2.2	Higher foaming temperatures	135
4.4	Conclusions	135

Chapter 5 Morphological, Mechanical, Thermal and Rheological Properties of SEBS Nanocomposites

5.1	Introduction	139
5.2	Effect of compositional variation	139
5.2.1	Nanocomposite sample preparation	139
5.2.2	DMA studies	140
5.2.3	Melt state dynamic rheology	143
5.2.4	Shear rheology	145
5.2.5	WAXD Studies	147
5.2.6	TEM studies	148
5.2.7	Thermal characterization	149
5.2.7.1	DSC studies	149
5.2.7.2	TGA studies	151
5.2.8	Tensile properties	152
5.3	Effect of screw speed	153
5.3.1	Nanocomposite sample preparation and residence time determination	153
5.3.2	Melt state rheology	154
5.3.3	Tensile properties	155
5.3.4	TEM studies	156
5.3.5	DMA studies	157
5.4	Conclusions	159
	<i>References</i>	159

Chapter 6 Foaming Behaviour of SEBS Nanocomposites

6.1	Introduction	164
6.2	Effect of compositional variation	164
6.2.1	Batch foaming	164
6.2.1.1	Shrinkage of foams with time	165
6.2.1.2	SEM studies of foams	168
6.2.1.2.1	Foaming temperature of 35 °C	169
6.2.1.2.1	Foaming temperature of 80 °C	170
6.3	Effect of screw speed	173
6.3.1	Batch foaming	173
6.3.1.1	Shrinkage of foams with time	173
6.3.1.2	SEM studies of foams	175
6.3.1.2.1	Foaming temperature of 35 °C	175
6.3.1.2.1	Foaming temperature of 80 °C	177
6.4	Foaming behaviour of nanocomposites of SEBS/PS blends	180
6.4.1	Sample preparation	180
6.4.2	DMA studies	181
6.4.3	Batch foaming	182
6.4.3.1	Volume expansion and shrinkage of foams	182
6.4.3.2	SEM studies of foams	183
6.5	Conclusions	184
	<i>References</i>	185

Chapter 7 Summary and Conclusions

7.1	Introduction	187
7.2	Summary	188
7.2.1	Morphological, mechanical, thermal and rheological properties of SEBS/PS blends	188
7.2.2	Foaming behaviour of SEBS/PS blends	189
7.2.3	Morphological, mechanical, thermal and rheological properties of SEBS nanocomposites	191
7.2.4	Foaming behaviour of SEBS nanocomposites	192
7.3	Conclusions	194
7.4	Future scope	196

List of Publications

Biography

List of Figures

Figure No.	Caption	Page Number
Figure 1.1	The different classes of TPEs	4
Figure 1.2	Structure of block copolymer type of TPE	5
Figure 1.3	Structure of montmorillonite	11
Figure 1.4	Types of morphology of polymer nanocomposites	12
Figure 1.5	Schematic representation of the foaming process	20
Figure 1.6	Schematic showing stages in extrusion foaming	24
Figure 1.7	Material characteristics influencing foaming behaviour	28
Figure 1.8	Summary of factors affecting the foaming behaviour of polymeric materials	42
Figure 3.1	SEM images at 10k \times magnification of (a) SEBS, (b) SEBS-10PS, (c) SEBS-20PS, (d) SEBS-30PS, and (e) SEBS-50PS	78
Figure 3.2	Cryo-fracturing of specimens (a) perpendicular to the direction of flow and (b) along the direction of flow	79
Figure 3.3	SEM images at 5k \times magnification of (a) SEBS, (b) SEBS-10PS, (c) SEBS-20PS, (d) SEBS-30PS and (e) SEBS-50PS extruded specimens cryo-fractured perpendicular to the direction of extrusion and stained	80
Figure 3.4	SEM images at 20k \times magnification of (a) SEBS-10PS, (b) SEBS-20PS, (c) SEBS-30PS and (d) SEBS-50PS extruded specimens cryo-fractured along the direction of extrusion and stained	81
Figure 3.5	SEM images at 10k \times magnification of (a) SEBS-10PS, (b) SEBS-20PS,	

	(c) SEBS-30PS and (d) SEBS-50PS moulded samples fractured perpendicular to direction of flow and stained	82
Figure 3.6	SEM images at 10k magnification of (a) SEBS-10PS, (b) SEBS-20PS, (c) SEBS-30PS and (d) SEBS-50PS moulded samples fractured parallel to the direction of flow and stained	82
Figure 3.7	Representative tensile curves of SEBS and blends having different PS Content	84
Figure 3.8	Comparison of the experimentally determined tensile modulus values of the blends with the predictions of models	87
Figure 3.9	Temperature dependence of (a) E' and (b) E'' of SEBS and blends having different PS content	89
Figure 3.10	DSC curves of SEBS and the blends having different PS content	90
Figure 3.11	TGA plots of SEBS and the blends having different PS content	93
Figure 3.12	Storage modulus and loss modulus plots of (a) SEBS, (b) SEBS-10PS, (c) SEBS-20PS, (d) SEBS-30PS, (e) SEBS-50PS and (f) PS	95
Figure 3.13	Weighted relaxation spectrum of SEBS and blends having different PS content	96
Figure 3.14	Schematic diagram of portion of micro-compounder having slit capillary back-flow channel which can be used for rheological studies.	97
Figure 3.15	MiniLab relative rheological measurements for SEBS and blends having different PS content	99
Figure 3.16	Complex viscosity curves of (a) SEBS and (b) PS at 200 °C and 210 °C	104
Figure 3.17	Frequency dependence at 200 °C of (a) storage modulus, (b) complex viscosity in the entire frequency range studied (c) complex viscosity in	

	the lower frequency region of the blends produced at different screw speeds	105
Figure 3.18	SEM images at 5k× magnification of (a) B50, (b) B100, (c) B200 and (d) B300	107
Figure 3.19	Representative tensile curves of SEBS and blends produced at different screw speeds	108
Figure 3.20	Temperature dependence of (a) E' and (b) E'' of blends produced at different screw speeds	109
Figure 4.1	Shrinkage of SEBS/PS blend foams produced at foaming temperatures of (a) 110 °C, (b) 100 °C, (c) 90 °C, (d) 80 °C and (e) 35 °C	118
Figure 4.2	Temperature dependence of complex viscosity of SEBS/PS blends	122
Figure 4.3	SEM images at 500X magnification of (a) SEBS, (b) SEBS-10PS, (c) SEBS-20PS, (d) SEBS-30PS and (e) SEBS-50PS foams produced at 35 °C	124
Figure 4.4	Cell size distribution graphs of (a) SEBS, (b) SEBS-10PS, (c) SEBS-20PS, (d) SEBS-30PS and (e) SEBS-50PS foams produced at 35 °C	125
Figure 4.5	SEM images at 10000× magnification of (a) SEBS, (b) SEBS-10PS, (c) SEBS-20PS, (d) SEBS-30PS and (e) SEBS-50PS foams produced at 35 °C	126
Figure 4.6	SEM images at 100× magnification of (a) SEBS, (b) SEBS-10PS, (c) SEBS-20PS, (d) SEBS-30PS and (e) SEBS-50PS foams produced at 100 °C	128
Figure 4.7	Variation of VE with time of foams produced at (a) 110 °C (b) 100 °C and (c) 35 °C	130

Figure 4.8	SEM images (2.5k magnification) of (a) B50 (b) B100 (c) B200 and (d) B300 foams produced at 35 °C	133
Figure 4.9	SEM images at 10k× magnification of (a) B50, (b) B100, (c) B200 and (d) B300 foams produced at 35 °C	134
Figure 4.10	Cell size distribution graphs of (a) B50, (b) B100, (c) B200 and (d) B300 foams produced at 35 °C	134
Figure 4.11	SEM images at 100× magnification of foams of (a) B50 (b) B100 (c) B200 and (d) B300 produced at 100 °C	135
Figure 5.1	Temperature dependence of (a) E' and (b) tan δ of SEBS and the nanocomposites	141
Figure 5.2	Storage modulus and loss modulus plots of (a) SEBS, (b) PNC-0.5, (c) PNC-1, (d) PNC-2 and (e) PNC-4	145
Figure 5.3	MiniLab relative rheological measurements for SEBS and the nanocomposites	147
Figure 5.4	WAXD patterns for Cloisite® 20A and the nanocomposites	148
Figure 5.5	TEM images of (a,e) PNC-0.5 (b,f) PNC-1 (c,g) PNC-2 and (d,h) PNC-4	148
Figure 5.6	DSC curves of SEBS and the nanocomposites	150
Figure 5.7	TGA plots of SEBS and the nanocomposites	151
Figure 5.8	Frequency dependence at 200 °C of (a) storage modulus and (b) complex viscosity of the nanocomposites produced at different screw speeds	155
Figure 5.9	TEM images of (a) NC100, (b) NC200 and (c) NC400	156
Figure 5.10	Temperature dependence of (a) E' and (b) tan δ of the nanocomposites produced at different screw speeds	157

Figure 6.1	Shrinkage of foams produced at foaming temperatures of (a) 80 °C and (b) 35 °C	165
Figure 6.2	SEM images at 500× magnification of (a) SEBS, (b) PNC-0.5, (c) PNC-1, (d) PNC-2 and (e) PNC-4 foams produced at 35 °C	169
Figure 6.3	Cell size distribution graphs of (a) SEBS, (b) PNC-0.5, (c) PNC-1, (d) PNC-2 and (e) PNC-4 foams produced at 35 °C	170
Figure 6.4	SEM images at 500× magnification of (a) SEBS, (b) PNC-0.5, (c) PNC-1, (d) PNC-2 and (e) PNC-4 foams produced at 80 °C	171
Figure 6.5	Cell size distribution graphs of (a) SEBS, (b) PNC-0.5, (c) PNC-1, (d) PNC-2 and (e) PNC-4 foams produced at 80 °C	172
Figure 6.6	Variation of VE with time of foams produced 80 °C	174
Figure 6.7	SEM images at 500× magnification of (a) NC100, (b) NC200 and (c) NC400 foams produced at 35 °C	175
Figure 6.8	Cell size distribution graphs of (a) NC100, (b) NC200 and (c) NC400 foams produced at 35 °C	176
Figure 6.9	SEM images at 500× magnification of (a) NC100, (b) NC200 and (c) NC400 foams produced at 80 °C	178
Figure 6.10	Cell size distribution graphs of (a) NC100, (b) NC200 and (c) NC400 foams produced at 80 °C	179
Figure 6.11	Temperature dependence of (a) E' and (b) E'' of SEBS/PS nanocomposites in comparison with SEBS/PS blends	181
Figure 6.12	SEM images at 100× magnification of (a) SEBS-30PS-NC, (b) SEBS-50PS-NC, (c) SEBS-30PS and (d) SEBS-50PS foams produced at 100 °C	183

List of Tables

Table No.	Caption	Page Number
Table 2.1	Details of SEBS grade used for studies	64
Table 2.2	Details of PS grade used for studies	65
Table 2.3	Details of SEBS-g-MA grade used for studies	65
Table 2.4	Details of C20A	66
Table 2.5	Compositions of SEBS/PS blends used for study	66
Table 2.6	Compositions of SEBS nanocomposites used for study	67
Table 3.1	Tensile properties of SEBS and the blends	85
Table 3.2	Comparison of T_g values obtained from DSC plots and DMA plots	91
Table 3.3	Degradation temperatures of SEBS and the blends	94
Table 3.4	Rheological parameters, shear viscosity and torque values	100
Table 3.5	Screw speeds, viscosity ratios and residence time	103
Table 3.6	Tensile properties and melt state rheological properties (at 0.01 Hz) of the blends	108
Table 4.1	Rheological properties of blend compositions and their foaming behavior at different temperatures	123
Table 4.2	Complex viscosity of the blends and shrinkage of their foams produced at different temperatures	132
Table 5.1	T_g values as determined from DMA studies of the nanocomposites	142
Table 5.2	Melt state dynamic rheological properties of the nanocomposites	144
Table 5.3	Rheological parameters of the nanocomposites in shear rheology	146
Table 5.4	Glass transition temperature(s) of nanocomposites obtained from DSC studies	150

Table 5.5	Degradation temperatures of SEBS and the nanocomposites	152
Table 5.6	Tensile properties of SEBS and the nanocomposites	152
Table 5.7	Screw speeds, viscosity ratios and residence time	154
Table 5.8	Tensile and melt state rheological properties (at 0.01 Hz) of the nanocomposites	156
Table 5.9	Glass transition temperature(s) from tan delta peak of nanocomposites produced at different screw speeds	158
Table 6.1	Shrinkage of nanocomposite foams produced at different temperatures	168
Table 6.2	Rheological properties of nanocomposite compositions and their foaming behavior at different temperatures	174
Table 6.3	Comparison of rheological and foam properties of SEBS/PS nanocomposites with those of SEBS/PS blends	182

List of Symbols

Symbol	Description
\bar{M}_n	: Number average molecular weight
\bar{M}_w	: Weight average molecular weight
T_g	: Glass transition temperature
ρ	: Density
T	: Torque
E	: Tensile modulus
Φ	: Volume fraction
τ	: Shear stress
$\dot{\gamma}$: Shear rate
η	: Shear viscosity
G'	: Storage modulus in melt state dynamic rheology
G''	: Loss modulus in melt state dynamic rheology
E'	: Storage modulus in DMA studies
E''	: Loss modulus in DMA studies
η^*	: Complex viscosity
ν	: Poisson's ratio
N_0	: Cell density

List of Abbreviations

Abbreviation	Description
TPE	: Thermoplastic elastomer
SEBS	: Styrene-ethylene-butylene-styrene
PS	: Polystyrene
C20A	: Cloisite® 20A
DSC	: Differential scanning calorimetry
TGA	: Thermal gravimetric analysis
DMA	: Dynamic mechanical analysis
SEM	: Scanning electron microscopy
TEM	: Transmission electron microscopy
WAXD	: Wide angle X-ray diffraction
VE	: Volume expansion ratio